Postprint of Journal of Functional Foods 26: 557-564 (2016)
http://dx.doi.org/10.1016/j.jff.2016.08.028

Olive oil, compared to a saturated dietary fat, has a protective role on atherosclerosis in niacin-treated mice with metabolic syndrome

Sergio **Montserrat-de la Paz**[a,*], Maria C **Naranjo**[a], Sergio **Lopez**[a], Rocio **Abia**[a], Francisco JG **Muriana**[a], Beatriz **Bermudez**[b,*]

[a] Laboratory of Cellular and Molecular Nutrition, Instituto de la Grasa, CSIC, Ctra. de Utrera Km. 1, 41013 Seville, Spain.

[b] Department of Cell Biology, School of Biology, University of Seville, C/ Profesor Garcia Gonzalez s/n, 41012 Seville, Spain.

Running title: MUFAs vs SFAs on atherosclerosis in NA-treated mice with MetS

*** Corresponding author:**
Sergio Montserrat-de la Paz, Beatriz Bermudez
Laboratory of Cellular and Molecular Nutrition, Instituto de la Grasa, CSIC.
Ctra. de Utrera Km. 1, Campus Universitario Pablo de Olavide, Edificio 46,
41013 Seville (Spain)
Tel: +34 954 611 550 (Ext. 360/359)
E-mail: delapaz@us.es, bbermudez@us.es

ABSTRACT

We aimed to investigate the impact of high-fat low-cholesterol diets rich in saturated fatty acids (HFLCD-SFAs), monounsaturated FAs (HFLCD-MUFAs) or MUFAs + omega-3 long-chain polyunsaturated FAs (HFLCD-PUFAs) in combination with niacin (NA) on atherosclerotic plaque characteristics in a mouse model ($Lep^{ob/ob}LDLR^{-/-}$) of metabolic syndrome (MetS). Compared to a low-fat low-cholesterol diet (LFLCD), HFLCDs increased body weight, triglycerides, insulin, pro-inflammatory cytokines, and circulating monocytes, contributing the HFLCD-SFAs to a predominance of a classical pro-inflammatory $Ly6C^{hi}$ population, whereas HFLCD-MUFAs and HFLCD-PUFAs to a non-classical patrolling $Ly6C^{lo}$ population. HFLCDs promoted atherosclerosis in the aortic roots of animals but the plaque size, collagen, and macrophage content were higher with the HFLCD-SFAs than with the HFLCD-MUFAs or HFLCD-PUFAs. Furthermore, HFLCD-SFAs promoted the intra-plaque accumulation of M1 macrophages, whereas HFLCD-MUFAs and HFLCD-PUFAs favoured the accumulation of M2 macrophages. These data suggest that dietary MUFAs had advantage over SFAs to prevent atherosclerotic events in the NA-treated MetS.

Keywords: Monounsaturated fatty acids; niacin; monocytes; atherosclerosis; macrophages; metabolic syndrome

1. Introduction

Dyslipidemia, insulin resistance, and obesity, the defining components of the metabolic syndrome (MetS), are well-known risk factors implicated in the aetiology and pathogenesis of certain cardiovascular diseases (CVDs) such as atherosclerosis, the main cause of CVD death in developed and some developing countries (Libby, 2012). Atherosclerosis is a systemic lipid-driven inflammatory condition associated with endothelial dysfunction that results in accumulation and subsequent oxidation of lipids in the vessel wall or plaque development. These abnormalities trigger inflammatory cell infiltration and macrophage foam cell formation leading to apoptosis and secondary necrosis and plaque advancement (Tabas, 2010). It is important to address the factors involved in the progression of atherosclerosis because advanced atherosclerotic lesions are prone to rupture, leading to disability or death. The monocyte-macrophage lineage is of fundamental interest in understanding atherosclerotic lesion progression (Ziegler-Heitbrock et al., 2010). Monocytes can be found into two distinct subsets based on the expression of specific surface markers. In mice, monocytes are divided based on Ly6C expression into inflammatory Ly6C high ($Ly6C^{hi}$) and patrolling Ly6C low ($Ly6C^{lo}$) monocytes (Auffray et al., 2007; Sunderkotter et al., 2004). CC-motif chemokine receptor 2 (CCR2) is expressed at high levels by inflammatory monocytes (Zlotnik & Yoshie, 2000), whereas CX_3C-motif chemokine receptor 1 (CX_3CR1) is more abundant on patrolling monocytes (Geissmann, Jung, & Littman, 2003; Woollard & Geissmann, 2010). Inflammatory monocytes are generally thought to be the most important subtype in early atherogenesis,

being efficiently recruited to the lesion in a CCR2-dependent manner (Robbins et al., 2012; Soehnlein et al., 2013).

The atheroprotective effects of niacin (NA), also known as nicotinic acid or vitamin B3, were first described in the 1950s (Carlson, 2005; Montserrat-de la Paz et al., 2016a). According to a meta-analysis of 30 randomized controlled trials, NA potently reduces triglycerides (TGs) by 15-30%, total cholesterol (TC) by 5-15%, and LDL-cholesterol (LDL-C) by 5-20% and increases HDL-cholesterol (HDL-C) by 10-25% in plasma of patients with dyslipidaemia and/or hypercholesterolemia (Birjmohun, Hutten, Kastelein, & Stroes, 2005). Additional to the pharmacology of NA, several translational studies have identified the differential role between saturated and unsaturated fats at cardiovascular level. Compared to saturated fatty acids (SFAs), the consumption of monounsaturated (MUFAs) and omega-3 long-chain polyunsaturated (PUFAs) fatty acids have beneficial effects on lowering blood lipids (Ortega et al., 2012; Vafeiadou et al., 2015) and inflammatory mediators (Naranjo et al., 2016;Teng, Chang, Chang, & Nesaretnam, 2014). However, the potential anti-atherogenic effects from a combination of dietary fatty acids and NA have not yet been defined. Therefore, the current study aimed to explore the influence of a pharmacological dose of NA and diets enriched in SFAs, MUFAs or MUFAs + omega-3 long-chain PUFAs on atherosclerosis in a mouse model ($Lep^{ob/ob}LDLR^{-/-}$) of MetS.

2. Materials and methods

2.1. Fatty acid composition of dietary fats

100 The fatty acid composition of dietary fats [cow's milk cream, rich in SFAs;
101 refined olive oil, rich in MUFAs; and refined olive oil plus eicosapentaenoic
102 acid (EPA) and docosahexaenoic acid (DHA), rich in MUFAs and omega-3
103 long-chain PUFAs] was determined by the method described in
104 EEC/796/2002 (Montserrat-de la Paz et al., 2016b), using a gas
105 chromatography system (HP-5890, Hewlett-Packard, Palo-Alto, USA)
106 equipped with flame ionization detector and a SP-2380 capillary column
107 (Supelco, Bellefonte, USA, 30 m x 0.32 mm) packed with cyanopropyl
108 siloxane (0.25 μm). The initial column temperature was 165 ºC, which was
109 held for 10 min, then programmed from 165 ºC to 200 ºC at 1.5 ºC/min.
110 Injector and detector temperature were 250 ºC, with the carrier gas H_2. The
111 fatty acid composition of different dietary fats is detailed in **Table 1**.
112
113 ***2.2. Animal diets and experimental design***
114 Male $Lep^{ob/ob}LDLR^{-/-}$ mice bred onto a C57BL/6J background (B6.Cg-Lepob
115 Ldlrtm1Her/J, The Jackson Laboratory, Bar Harbor, ME, USA) was used for
116 the study. These mice are obese and develop plasma lipid alterations that
117 closely reflect MetS-related hyperlipidaemia (Kennedy et al., 2010;
118 Montserrat-de la Paz et al., 2016c). All diets were prepared by Panlab
119 Laboratoires (SAFE, Augy, France) and presented as pellets to the animals.
120 Mice received one of the following diets for 8 weeks: a standard normal-fat
121 diet (low-fat low-cholesterol diet, LFLCD) containing 3% energy as fat, used
122 as control, or high-fat low-cholesterol diets (HFLCDs), which contained 24%
123 energy as fat. All the diets were based on the standard rodent diet A04-10,
124 containing 0.01% cholesterol, 20 mg/kg BHT, and 3% binder. Three different

HFLCDs were prepared by replacing the fat source from A04-10 diet by cow's milk cream (21% energy) (HFLCD-SFAs), refined olive oil (21% energy) (HFLCD-MUFAs) or refined olive oil (20% energy) plus EPA+DHA in the form of ethyl esters (1% energy) (HFLCD-PUFAs). The cow's milk cream provided an additional amount of 0.006% by weight. All the diets contained equal proportion of protein (19.5% energy) and carbohydrate was used to adjust the total energy content.

After weaning, mice were randomly allocated into 4 groups (n = 10 per group) as follows: (1) group that received LFLCD; (2) group that received HFLCD-SFAs; (3) group that received HFLCD-MUFAs; and (4) group that received HFLCD-PUFAs. The four groups received NA (1%, w/v; Twinlab, UT, USA) in the drinking water. Body weight, food, and water intake were daily evaluated. Sacrifice of all animals was carried out within the animal facilities (Instituto de Biomedicina de Sevilla, IBiS), at the beginning of the light cycle and after 10 h of food deprivation. Animals were euthanized with an overdose of pentobarbital (1:10 in PBS, 150 mg/kg body weight). Cardiac puncture was used to blood collection. Heart samples were collected upon sacrifice. All animal protocols received appropriate institutional approval (Animal Care and Use Committee of the University of Seville) and were performed according to the official rules formulated in the Spanish law on the care and use of experimental animals (UE Directive of 2010: 2010/63/UE; RD 53/2013).

2.3. Biochemical parameters

149 Serum samples were obtained from blood by centrifugation at 1800 *g* for 15
150 min at 4 ºC. Fasting serum levels of glucose, TC, and TGs were assessed by
151 colorimetric assay kits (Bio-science-medical, Madrid, Spain). Serum cytokines
152 were measured using Multiplex Biomarker Immunoassays for Luminex xMAP
153 technology (Millipore, Billerica, USA).
154
155 ***2.4. Immunostaining of circulating monocytes by FACS***
156 Cardiac blood samples were collected at the end of each dietary period.
157 Circulating monocyte membrane expression of CD11b (PerpCy5.5 anti-mouse
158 CD11b, Becton Dickinson, Oxford, UK), Ly6G (FITC anti-mouse Ly6G,
159 Miltenyi, Madrid, Spain), Ly6C (APC-Cy7 anti-mouse Ly6C, Miltenyi), CCR2
160 (APC anti-mouse CCR2, Miltenyi), and CX_3CR1 (PE-Cy7 anti-mouse
161 CX_3CR1, BD) was assessed by flow cytometry. Cells were incubated with
162 antibodies at room temperature, in the dark, for 15 min, followed by fixation
163 and lysing of erythrocytes with 20× volume of Fluorescence Activated Cell
164 Sorting (FACS) lysing solution (BD). Fluorescence intensity was measured by
165 using a FACSCanto II cytometer and calibrated using FACSCanto II Cell
166 analyser software (BD). Mean fluorescence intensity (MFI) of 10^4 counted
167 cells was measured in each sample. Monocytes were gated as forward
168 $scatter^{high}$ (FSC^{hi})-side $scatter^{high}$ (SSC^{hi})-cells. Expression levels were
169 presented as MFI corrected for nonspecific binding of isotype control
170 antibodies.
171
172 ***2.5. Immunohistochemistry***

Mouse heart was dissected, fixed in 1% paraformaldehyde, and embedded in paraffin. Size of atherosclerotic lesions was determined as previously described (Gijbels et al., 1999). Serial sections (6 μm) of the aortic root were cut and stained with haematoxylin-eosin (HE) for morphometric analysis and routine qualitative examination of collagen content, necrosis, and amount of inflammatory B (B220) and C (CD3) cells. Sirius Red was used for the detection of collagen. A polarized filter and birefringence colour discrimination was used to differentiate various collagen structures [ranging from loosely patched, immature, thin collagen (green) to tightly packed, mature, thick collagen fibres (red)] as previously described (Mackenna, Omens, & Covell, 1996). For evaluation of macrophage content were used MAC3 (an antibody recognizing pan macrophages), CCR7 (antibody against M1 macrophages), and CD163 (antibody against M2 macrophages). Samples were captured at 20× magnifications by a Leica DM3000 light microscope (Leica, Wetzlar, Germany) and an independent operator, in a blinder manner, performed histological analyses using Quantimet with Qwin3 quantification software (Leica).

2.6. Statistical analysis

All values in the figures and text are expressed as the arithmetic mean ± SD. Experiments were carried out in triplicate. Data were evaluated with Graph Pad Prism Version 5.01 software. The statistical significance of any difference in each parameter among the groups was evaluated by one-way analysis of variance (ANOVA), using Tukey's test for multiple comparison analysis. *P* values of <0.05 were considered statistically significant.

198

199 ## 3. Results

200 ### *3.1. MUFA-rich diets reduce body weight gain and serum TG, insulin,*

201 ### *and pro-inflammatory cytokine levels compared to the SFA-rich diet in*

202 ### *NA-treated Lep$^{ob/ob}$LDLR$^{-/-}$ mice*

203 In the setting of NA treatment, mean daily food intake (LFLCD, 4.07 ± 0.32;
204 HFLCD-SFAs, 4.15 ± 0.61; HFLCD-MUFAs, 4.01 ± 0.47; HFLCD-PUFAs,
205 4.17 ± 0.41 g/mouse) and water intake (LFLCD, 6.28 ± 0.83; HFLCD-SFAs,
206 6.35 ± 1.01; HFLCD-MUFAs, 6.12 ± 0.77; HFLCD-PUFAs, 6.11 ± 0.81
207 mL/mouse) were not different among the four diet groups. Despite similarities
208 in food and drink intake, the final body weight and body weight gain of animals
209 increased but to a different degree depending on the diet (HFLCD-SFAs >
210 HFLCD-MUFAs = HFLCD-PUFAs > LFLCD, **Table 2**). Serum TG levels were
211 significantly higher in animals fed with HFLCDs (HFLCD-SFAs > HFLCD-
212 MUFAs = HFLCD-PUFAs) than in those fed with the LFLCD. Serum TC levels
213 did not differ among the HFLCD groups but were higher than those observed
214 in the LFLCD group. Notably, serum insulin levels were significantly different
215 in all groups: HFLCD-SFAs > HFLCD-MUFAs > HFLCD-PUFAs > LFLCD. No
216 differences were observed for serum glucose levels. In relation to pro-
217 inflammatory cytokines, serum TNF-α levels were higher only in animals fed
218 with HFLCD-SFAs, whereas serum IL-6 and monocyte chemoattractant
219 protein-1 (MCP-1/CCL2) levels were found to be higher in animals fed with
220 HFLCDs (for IL-6, HFLCD-SFAs > HFLCD-MUFAs = HFLCD-PUFAs; for
221 MCP-1, HFLCD-SFAs = HFLCD-MUFAs = HFLCD-PUFAs) than in those fed
222 with the LFLCD.

3.2. MUFA-rich diets skew the frequency of circulating monocytes toward a CD11b^{+}Ly6G^{lo}Ly6C^{lo}CX$_3$CR1^{hi} patrolling subset compared to the SFA-rich diet in NA-treated Lep$^{ob/ob}$LDLR$^{-/-}$ mice

We examined the effects of the different diets on blood monocyte activation. CD11b^{+}Ly6G^{lo} monocytes were gated on Ly6C expression (**Figure 1A**). Animals on HFLCDs had a significant increase (P<0.05) of total circulating monocytes (960000 ± 109000 per mL after the HFLCD-SFAs; 900000 ± 80000 per mL after the HFLCD-MUFAs; 920000 ± 100000 per mL after the HFLCD-PUFAs) when compared to animals fed with the LFLCD (600000 ± 30000 monocytes/mL). This monocytosis resulted from a 60% of Ly6C^{lo} subset after HFLCD-MUFAs and HFLCD-PUFAs (**Figure 1B**) and a 60% of Ly6C^{hi} subset after the HFLCD-SFAs (data not shown). As depicted in **Figure 1C**, total monocyte population from animals fed with HFLCD-MUFAs and HFLCD-PUFAs had increased CX$_3$CR1 expression. These monocytes also had lower CCR2 expression than those of animals fed with the HFLCD-SFAs (**Figure 1D**).

3.3. MUFA-rich diets lead to a lesser atherosclerotic lesion size and collagen content compared to the SFA-rich diet in NA-treated Lep$^{ob/ob}$LDLR$^{-/-}$ mice

All of the HFLCDs induced plaque formation in aortic roots of animals when compared to the LFLCD, but this effect was more marked with the HFLCD-SFAs than with HFLCD-MUFAs or HFLCD-PUFAs (**Figure 2A**). After HFLCD-MUFAs and HFLCD-PUFAs, the plaque size by means of HE staining was

248 half the plaque size after the HFLCD-SFAs (**Figure 2B**). Atherosclerotic
249 lesions were further examined for collagen and adventitial inflammatory cell
250 content and for necrosis. Any atherosclerotic plaque had necrosis or
251 adventitial infiltration of inflammatory cells (data not shown). However, the
252 fibrosis by means of collagen content was dramatically increased in plaques
253 of animals fed with HFLCDs (**Figures 3A** and **3B**). Interestingly, HFLCD-
254 MUFAs and HFLCD-PUFAs induced plaques with half of collagen deposited
255 in those induced by the HFLCD-SFAs (**Figure 3C**). Differentiating on the
256 basis of collagen structure [loosely patched, immature, thin collage (green)
257 versus tightly packed, mature, thick collagen fibres (red)] by using a
258 polarization filter (**Figure 3B**), we observed that increased plaque fibrosis with
259 the HFLCD-SFAs was concomitant with an increase in mature, thick collagen
260 fibre content (**Figure 3D**).
261
262 ***3.4. MUFA-rich diets favour alternatively activated macrophages in***
263 ***atherosclerotic plaques compared to the SFA-rich diet in NA-treated***
264 ***Lep$^{ob/ob}$LDLR$^{-/-}$ mice***
265 Macrophage accumulation and phenotype in atherosclerotic plaques of
266 animals fed with the different diets were determined by immunohistochemical
267 staining of MAC3 (pan-macrophage marker) (**Figure 4A**), CCR7 (M1
268 macrophage marker) (**Figure 4B**), and CD163 (M2 macrophage marker)
269 (**Figure 4C**). It was noteworthy to observe a markedly increased accumulation
270 of macrophages (**Figure 4D**), mainly of type M1 (**Figure 4E**), in plaques from
271 animals fed with the HFLCD-SFAs. However, HFLCD-MUFAs and HFLCD-

PUFAs promoted the intra-plaque accumulation of M2 macrophages when compared to the HFLCD-SFAs or LFLCD (**Figure 4F**).

4. Discussion

This study is the first to address the effects of predominant fatty acids in dietary fats and NA co-ingestion on atherosclerosis in mice. We used male mice homozygous for the *ob/ob* and *Ldlr*^{tm1Her} targeted mutations lacking the hormone leptin and LDL receptor onto a C57BL/6J background. When subjected to a HFLCD rich in SFAs, these animals become obese, hyperinsulinemic, and develop severe dyslipidaemia, which are pathological manifestations analogous to those characteristics of human MetS (Git & Adan, 2015; Kennedy et al., 2010). In the setting of NA treatment, we demonstrate that compared to dietary SFAs, dietary MUFAs, accompanied or not with omega-3 long-chain PUFAs, confer atheroprotection by impacting on several hallmark processes directly associated with atherosclerosis: MUFAs + NA induced a less inflammatory cytokine profile; MUFAs + NA induced a mobilization of less inflammatory monocytes; MUFAs + NA favourably altered plaque size, fibrosis, and M1/M2 phenotype of recruited macrophages. In addition, the gain of body weight with HFLCDs rich in MUFAs was attended by lower serum lipid and insulin levels than with the HFLCD rich in SFAs, suggesting that MUFAs + NA also ameliorated some of the metabolic complications of the HFLCD-induced obesity.

The persistence of circulating pro-inflammatory cytokines and chemokines may be harmful at multiple levels and at different stages of atherosclerosis

297 from early to advanced disease (Ait-Oufella et al., 2011). In contrast to the
298 HFLCD rich in SFAs, we found that HFLCDs rich in MUFAs did not alter
299 serum TNF-α levels and minimally increased serum IL-6 and MCP-1 levels. A
300 decrease in the production of TNF-α in atherosclerosis-prone mice has been
301 reported to diminish the extent of anatomic lesions, even the expression of
302 MCP-1 in atherosclerotic vessels (Ohta et al., 2005). MCP-1 is one of the key
303 chemokines that regulate migration and infiltration of monocytes, memory T
304 lymphocytes, and natural killer cells (Deshmane et al., 2009). Therefore, our
305 findings, in accordance with previous studies showing the anti-inflammatory
306 benefits of dietary MUFAs (Finucane et al., 2015; Ortega et al., 2012) and NA
307 (Lipszyc et al., 2013) separately, suggest that dietary MUFAs + NA may be
308 atheroprotective in the MetS by contributing to a reduced inflammatory status
309 and recruitment of leukocytes into the plaque.
310
311 Monocyte-derived macrophages are the most abundant myeloid cell type in
312 atherosclerotic lesions (Hilgendorf, Swirski, & Robbins, 2015). The higher the
313 number of circulating monocytes increases the risk of monocyte priming-
314 activation and accumulation at sites of inflammation. Prolonged exposure to
315 hypercholesterolemia has been reported to influence on hematopoietic stem
316 and multipotential progenitor cells in the bone marrow, leading to over-
317 production of monocytes (Soehnlein & Swirski, 2013; Tolani et al., 2013) and
318 pointing to a link between haematopoietic hyperactivity with the
319 atherosclerotic lesion burden (van der Valk et al., 2016). We observed that
320 HFLCDs rich in MUFAs induced monocytosis but to a lower extent than the
321 HFLCD rich in SFAs. This effect was unlikely due to serum cholesterol levels,

as they did not differ among the HFLCDs. Whether triglyceride or fatty acid sensing pathways, in combination with NA (Montserrat-de la Paz et al., 2016c), orchestrate myelopoiesis requires further investigations. It was also interesting to observe that HFLCDs rich in MUFAs retained the phenotype of circulating monocytes with a preponderance of the Ly6C^{lo} subset, which displays a reduced capacity for plaque invasion and a preferential polarization into M2 macrophages (Moore, Sheedy, & Fisher, 2013). These Ly6C^{lo} monocytes were featured by a marked accumulation of the fractalkine receptor CX_3CR1. While all monocytes constitutively express CX_3CR1, those expressing the highest levels of CX_3CR1 belong to the non-classical monocyte subset that barely express the chemoattractant CCR2 (Ancuta et al., 2003), that actively keep survival signals under both steady-state and inflammatory conditions (Landsman et al., 2009), and that specifically participate in wound healing and the resolution of inflammation (Thomas, Tacke, Hedrick, & Hanna, 2015). In keeping with this notion, atherosclerotic plaques in animals fed with HFLCDs rich in MUFAs had lower number of macrophages, much of which exhibiting the M2 phenotype, smaller size, and less collagen deposition than in animals fed with the HFLCD rich in SFAs. Importantly, despite the HFLCD-associated monocyte expansion, these observations and the reduced monocyte expression of CCR2, which is utilized to enter lesions (Gui, Shimokado, Sun, Akasaka, & Muragaki, 2012; Moore, Sheedy, & Fisher, 2013), are indicative of a prominent role for dietary MUFAs + NA in retaining the abundance of circulating resident/reparative/patrolling or non-classical monocytes and in lowering the traffic of myeloid cells to plaque and the intra-plaque inflammatory environment.

5. Conclusion

Our study demonstrates that compared to dietary SFAs, MUFAs from olive oil in combination with NA prevent against atherosclerosis by interfering on different hallmark events at several independent levels in the setting of MetS.

Conflicts of interest

The authors state no conflict of interest

Acknowledgements

This study was supported by the research Grant AGL2011-29008 (Spanish Ministry of Science and Innovation, MICINN). S.M. has the benefit of a FPI fellowship (BES-2012-056104) of MICINN. B.B. and S.L. acknowledge financial support from “V Own Research Plan” (University of Seville) and the Spanish Research Council (CSIC)/Juan de la Cierva, respectively.

REFERENCES

Ait-Oufella, H., Taleb, S., Mallat, Z., & Tedgui, A. (2011). Recent advances on the role of cytokines in atherosclerosis. *Arteriosclerosis, Thrombosis, and Vascular Biology, 31,* 969-979.

Ancuta, P., Rao, R., Moses, A., Mehle, A., Shaw, S.K., Luscinskas, F.W., & Gabuzda, D. (2003). Fractalkine preferentially mediates arrest and migration of CD16+ monocytes. *Journal of Experimental Medicine, 197,* 1701-1707.

Auffray, C., Fogg, D., Garfa, M., Elain, G., Join-Lambert, O., Kayal, S., Sarnacki, S., Cumano, A., Lauvau, G., & Geissmann, F. (2007). Monitoring of blood vessels and tissues by a population of monocytes with patrolling behavior. *Science*, *317*, 666-670.

Birjmohun, R.S., Hutten, B.A., Kastelein, J.J., & Stroes, E.S. (2005). Efficacy and safety of high-density lipoprotein cholesterol-increasing compounds: a meta-analysis of randomized controlled trials. *Journal of American College of Cardiology*, *45*, 185–197.

Carlson, L.A. (2005). Nicotinic acid: the broad-spectrum lipid drug. A 50th anniversary review. *Journal of Internal Medicine*, *258,* 94–114.

Deshmane, S.L., Kremlev, S., Amini, S., & Sawaya, B.E. (2009). Monocyte chemoattractant protein-1 (MCP-1): an overview. *Journal of Interferon & Cytokine Research,* 29, 313-326.

Finucane, O.M., Lyons, C.L., Murphy, A.M., Reynolds, C.M., Klinger, R., Healy, N.P., Cooke, A.A., Coll, R.C., McAllan, L., Nilaweera, K.N., et al. (2015). Monounsaturated fatty acid-enriched high-fat diets impede adipose NLRP3 inflammasome-mediated IL-1β secretion and insulin resistance despite obesity. *Diabetes, 64*, 2116-2128.

Geissmann, F., Jung, S., & Littman, D.R. (2003). Blood monocytes consist of two principal subsets with distinct migratory properties. *Immunity*, *19*, 71-82.

Gijbels, M.J., van der Cammen, M., van der Laan, L.J., Emeis, J.J., Havekes, L.M., Hofker, M.H., & Kraal, G. (1999). Progression and regression of atherosclerosis in apoe3-leiden transgenic mice: An immunohistochemical study. *Atherosclerosis, 143,* 15-25.

Git, K.C., & Adan R.A. (2015). Leptin resistance in diet-induced obesity: the role of hypothalamic inflammation. *Obesity Reviews, 16*, 207-224.

Gui, T., Shimokado, A., Sun, Y., Akasaka, T., & Muragaki, Y. (2012). Diverse roles of macrophages in atherosclerosis: From inflammatory biology to biomarker discovery. *Mediators of Inflammation, 2012,* 693083.

Hilgendorf, I., Swirski, F.K., & Robbins, C.S. (2015). Monocyte fate in atherosclerosis. *Arteriosclerosis, Thrombosis, and Vascular Biology, 35,* 272-279.

Kennedy, A.J., Ellacott, K.L.J., King, V.L., & Hasty, A.H. (2010). Mouse models of the metabolic syndrome. *Disease Models & Mechanisms*, *3,* 156-166.

Landsman, L., Bar-On, L., Zernecke, A., Kim, K.W., Krauthgamer, R., Shagdarsuren, E., Lira, S.A., Weissman, I.L., Weber, C., & Jung, S. (2009). CX3CR1 is required for monocyte homeostasis and atherogenesis by promoting cell survival. *Blood, 113,* 963-972.

Libby, P. (2012). Inflammation in atherosclerosis. *Arteriosclerosis, Thrombosis, & Vascular Biology,* 32, 2045–2051.

Lipszyc, P.S., Cremaschi, G.A., Zorrilla-Zubilete, M., Bertolino, M.L., Capani, F., Genaro, A.M., & Wald, M.R. (2013). Niacin Modulates Pro-inflammatory

Cytokine Secretion. A Potential Mechanism Involved in its Anti-atherosclerotic Effect. *Open Cardiovascular Medicine Journal, 7,* 90-98.

Mackenna, D.A., Omens, J.H., & Covell, J.W. (1996). Left ventricular perimysial collagen fibers uncoil rather than stretch during diastolic filling. *Basic Research in Cardiology, 91*, 111-122.

Montserrat-de la Paz, S., Bermudez, B., Naranjo, M.C., Lopez, S., Abia, R., & Muriana, F.J.G. (2016a). Pharmacological effects of niacin on acute hyperlipemia. *Current Medicinal Chemistry* (Epub ahead of print)

Montserrat-de la Paz, S., Naranjo, M.C., Bermudez, B., Lopez, S., Moreda, W., Abia, R., & Muriana, F.J. (2016b). Postprandial dietary fatty acids exert divergent inflammatory responses in retinal-pigmented epithelium cells. *Food & Function, 7,* 1345-1353.

Montserrat-de la Paz, S., Naranjo, M.C., Lopez, S., Abia, R., Muriana, F.J., & Bermudez, B. (2016c). Niacin and olive oil promote skewing to the M2 phenotype in bone marrow-derived macrophages of mice with metabolic syndrome. *Food & Function, 7,* 2233-2238.

Moore, K.J., Sheedy, F.J., & Fisher, E.A. (2013). Macrophages in atherosclerosis: a dynamic balance. *Nature Reviews in Immunology, 13,* 709-721.

Naranjo, M.C., Garcia, I., Bermudez, B., Lopez, S., Cardelo, M.P., Abia, R., Muriana, F.J.G., & Montserrat-de la Paz, S. (2016). Acute effects of dietary fatty acids on osteoclastogenesis via RANKL/RANK/OPG system. *Molecular Nutrition & Food Research* doi: 10.1002/mnfr.201600303

Ohta, H., Wada, H., Niwa, T., Kirii, H., Iwamoto, N., Fujii, H., Saito, K., Sekikawa, K., & Seishima, M. (2005). Disruption of tumor necrosis factor-

alpha gene diminishes the development of atherosclerosis in ApoE-deficient mice. *Atherosclerosis, 180,* 11-17.

Ortega, A., Varela, L.M., Bermudez, B., Lopez, S., Abia, R., & Muriana, F.J. (2012). Dietary fatty acids linking postprandial metabolic response and chronic diseases. *Food & Function*, *2,* 22-27.

Robbins, C.S., Chudnovskiy, A., Rauch, P., Figuereido, J.L., Iwamoto, Y., Gorbatov, R., Etzrodt, M., Weber, G.F., Ueno, T., van Rooijen, N., *et al.* (2012). Extremedullary hematopoiesis generates Ly-6C(high) monocytes that infiltrate atherosclerotic lesions. *Circulation*, *125,* 364-374.

Soehnlein, O., Drechsler, M., Doring, Y., Lievens, D., Hartwig, H., Kemmerich, K., Ortega-Gomez, A., Mandl, M., Vijayan, S., Projahn, D., *et al.* (2013). Distinct functions of chemokine receptor axes in the atherogenic mobilization and recruitment of classical monocytes. *EMBO Molecular Medicine*, *5*, 471–481.

Soehnlein, O., & Swirski, F.K. (2013). Hypercholesterolemia links hematopoiesis with atherosclerosis. *Trends in Endocrinology and Metabolism, 24,* 129-136.

Sunderkotter, C., Nikolic, T., Dillon, M.J., Van Rooijen, N., Stehling, M., Drevets, D.A., & Leenen, P.J. (2004). Subpopulations of mouse blood monocytes differ maturation stage and inflammatory response. *Journal of Immunology, 172*, 4410-4417.

Tabas, I. (2010) Macrophage death and defective inflammation resolution in atherosclerosis. *Nature Review in Immunology, 10,* 36-46.

Teng, K.T., Chang, C.Y., Chang, L.F., & Nesaretnam, K. (2014). Modulation of obesity-induced inflammation by dietary fats: mechanisms and clinical evidence. *Nutrition Journal*, *13,* 12.

Thomas, G., Tacke, R., Hedrick, C.C., & Hanna, R.N. (2015). Nonclassical patrolling monocyte function in the vasculature. *Arteriosclerosis, Thrombosis, and Vascular Biology, 35,* 1306-1316.

Tolani, S., Pagler, T.A., Murphy, A.J., Bochem, A.E., Abramowicz, S., Welch, C., Nagareddy, P.R., Holleran, S., Hovingh, G.K., Kuivenhoven, J.A., et al. (2013). Hypercholesterolemia and reduced HDL-C promote hematopoietic stem cell proliferation and monocytosis: studies in mice and FH children. *Atherosclerosis, 229,* 79-85.

Vafeiadou, K., Weech, M., Altowaijri, H., Todd, S., Yaqoob, P., Jackson, K.G., & Lovegrove, J.A. (2015). Replacement of saturated with unsaturated fats had no impact on vascular function but beneficial effects on lipid biomarkers, E-selectin, and blood pressure: results from the randomized, controlled Dietary Intervention and VAScular function (DIVAS) study. *American Journal of Clinical Nutrition*, *102,* 40-48.

van der Valk, F.M., Kuijk, C., Verweij, S.L., Stiekema, L.C., Kaiser, Y., Zeerleder, S., Nahrendorf, M., Voermans, C., & Stroes, E.S. (2016). Increased haematopoietic activity in patients with atherosclerosis. *European Heart Journal* (Epub ahead of print)

Woollard, K.J., & Geissmann, F. (2010). Monocytes in aterosclerosis: subsets and functions. *Nature Review in Cardiology*, *7*, 77-86.

Ziegler-Heitbrock, L., Ancuta, P., Crowe, S., Dalod, M., Grau, V., Hart, D.N., Leenen, P.J., Liu, Y.J., MacPherson, G., Randolph, G.J., *et al.* (2010). Nomenclature of monocytes and dendritic cells in blood. *Blood*, *116*, e74-80.

Zlotnik, A., & Yoshie, O. (2000). Chemokines: a new classification system and their role in immunity. *Immunity*, *12*, 121-127.

Figure Legends

Figure 1. (**A**) Representative FACS plots showing the gating strategy to identify and quantify the circulating monocyte populations, (**B**) percentage of Ly6C^{lo} monocytes over total circulating monocytes, (**C**) CX_3CR1 and (**D**) CCR2 expression (MFI, mean fluorescence intensity) in total circulating monocytes in Lep$^{ob/ob}$LDLR$^{-/-}$ mice treated with NA and fed with LFLCD, HFLCD-SFAs, HFLCD-MUFAs, and HFLCD-PUFAs during 8 weeks. Values are presented as the mean ± SD (n = 10) and those marked with different lowercase letter are statistically different ($P < 0.05$).

Figure 2. (A) Representative pictures of HE stained sections (original magnification ×40) and (**B**) quantification of aortic root plaque area in Lep$^{ob/ob}$LDLR$^{-/-}$ mice treated with NA and fed with LFLCD, HFLCD-SFAs, HFLCD-MUFAs, and HFLCD-PUFAs during 8 weeks. Scale bar is applicable to all pictures of the panel (A). Values are presented as the mean ± SD (n = 10) and those marked with different lowercase letter are statistically different ($P < 0.05$).

Figure 3. Representative pictures of Sirius Red stained sections (original magnification ×40) of aortic root plaque area examined by normal light (**A**) and polarized (**B**) microscopy, (**C**) percentage of collagen in aortic root plaque area, and (**D**) quantification of different collagen fibres per unit of aortic root plaque area in Lep$^{ob/ob}$LDLR$^{-/-}$ mice treated with NA and fed with LFLCD, HFLCD-SFAs, HFLCD-MUFAs, and HFLCD-PUFAs during 8 weeks. Values

542 are presented as the mean ± SD (n = 10) and those marked with different
543 lowercase letter are statistically different ($P < 0.05$).
544
545 **Figure 4.** Representative pictures of immunohistochemically stained sections
546 (original magnification ×40) for (**A**) MAC3, (**B**) CCR7, and (**C**) CD163 positive
547 cells, and percentage of (**D**) total, (**E**) M1, and (**F**) M2 macrophages in aortic
548 root plaque area of $Lep^{ob/ob}LDLR^{-/-}$ mice treated with NA and fed with LFLCD,
549 HFLCD-SFAs, HFLCD-MUFAs, and HFLCD-PUFAs during 8 weeks. Values
550 are presented as the mean ± SD (n = 10) and those marked with different
551 lowercase letter are statistically different ($P < 0.05$).

Table 1. Fatty acid composition of dietary fats.

	Cow's milk cream	Refined olive oil	Refined olive oil plus EPA + DHA
Fatty acid		**g/100 g of fatty acid**	
10:0, capric	2.5 ± 0.1	-	-
12:0, lauric	3.1 ± 0.4	-	-
14:0, myristic	10.9 ± 0.9	-	-
16:0, palmitic	35.5 ± 0.8	20.4 ± 0.9	20.5 ± 0.6
16:1(n-7), palmitoleic	3.6 ± 0.3	1.0 ± 0.2	0.8 ± 0.1
18:0, stearic	11.5 ± 0.8	5.7 ± 0.1	4.5 ± 0.4
18:1(n-9), oleic	25.3 ± 0.7	61.9 ± 1.2	61.5 ± 1.0
18:2(n-6), linoleic	4.3 ± 0.8	8.0 ± 0.7	8.0 ± 0.5
18:3(n-3), α-linolenic	0.4 ± 0.1	1.0 ± 0.1	0.9 ± 0.0
20:5(n-3), eicosapentaenoic	-	-	0.9 ± 0.1
22:6(n-3), docosahexaenoic	-	-	0.7 ± 0.1
Others	3.0 ± 1.7	2.1 ± 1.1	2.0 ± 0.9
SFAs	63.5 ± 1.9[a]	26.1 ± 1.0[b]	25.0 ± 0.9[b]
MUFAs	28.9 ± 0.8[b]	62.8 ± 1.4[a]	62.4 ± 1.0[a]
PUFAs	4.7 ± 0.8[c]	9.0 ± 0.7[b]	10.6 ± 0.7[a]

Values are expressed as the mean ± SD (n = 3) and those marked with different lowercase letter in the same row are statistically different (P < 0.05).

Table 2. Food intake, final body and relative weights, and biochemical blood analysis of $Lep^{ob/ob}LDLR^{-/-}$ mice treated with NA and fed with LFLCD, HFLCD-SFAs, HFLCD-MUFAs, and HFLCD-PUFAs during 8 weeks.

	LFLCD	**HFLCD-SFAs**	**HFLCD-MUFAs**	**HFLCD-PUFAs**
Food intake (g/wk/animal)	26.2 ± 4.4^{a}	32.8 ± 7.6^{a}	29.6 ± 10.6^{a}	31.77 ± 7.4^{a}
Final body weight (g)	28.6 ± 2.7^{c}	38.5 ± 2.3^{a}	32.4 ± 1.1^{b}	31.7 ± 1.8^{b}
Body weight gain (g)	9.0 ± 0.7^{c}	18.4 ± 1.6^{a}	11.7 ± 0.3^{b}	11.0 ± 1.1^{b}
Biochemical blood parameters				
TC (mmol/L)	3.6 ± 0.2^{b}	4.3 ± 0.3^{a}	4.1 ± 0.2^{a}	4.0 ± 0.1^{a}
TGs (mmol/L)	0.4 ± 0.1^{c}	0.8 ± 0.1^{a}	0.5 ± 0.1^{b}	0.5 ± 0.1^{b}
Glucose (mg/dL)	138.2 ± 6.7^{a}	147.5 ± 4.9^{a}	143.8 ± 7.3^{a}	151.5 ± 4.9^{a}
Insulin (pg/mL)	412.5 ± 92.0^{d}	1103.7 ± 105.1^{a}	873.3 ± 82.7^{b}	707.3 ± 92.2^{c}
TNF-α (pg/mL)	4.0 ± 0.2^{b}	4.7 ± 0.2^{a}	4.2 ± 0.1^{b}	4.2 ± 0.1^{b}
IL-6 (pg/mL)	2.9 ± 0.2^{c}	9.7 ± 1.0^{a}	5.0 ± 0.4^{b}	4.7 ± 0.3^{b}
MCP-1 (pg/mL)	32.9 ± 2.3^{b}	41.0 ± 3.3^{a}	38.2 ± 2.1^{a}	38.4 ± 2.7^{a}

Values are expressed as the mean ± SD (n = 10) and those marked with different lowercase letter in the same row are statistically different ($P < 0.05$).

Figure 1

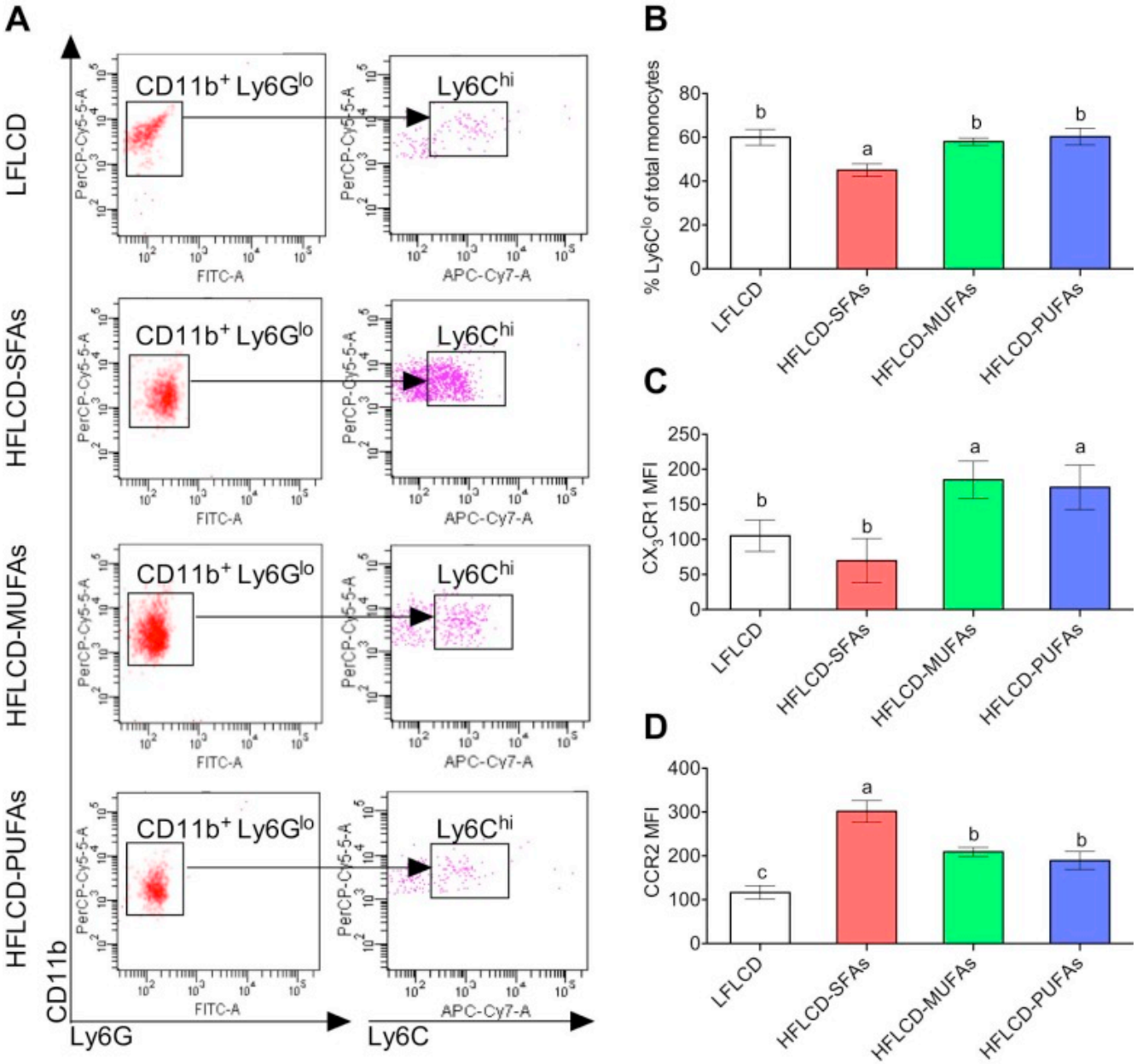
A
LFLCD
HFLCD-SFAs
HFLCD-MUFAs
HFLCD-PUFAs
CD11b+ Ly6Glo
Ly6Chi
PerCP-Cy5-5-A
FITC-A
APC-Cy7-A
CD11b
Ly6G
Ly6C
B
% Ly6Clo of total monocytes
C
CX3CR1 MFI
D
CCR2 MFI
LFLCD
HFLCD-SFAs
HFLCD-MUFAs
HFLCD-PUFAs

Figura 2

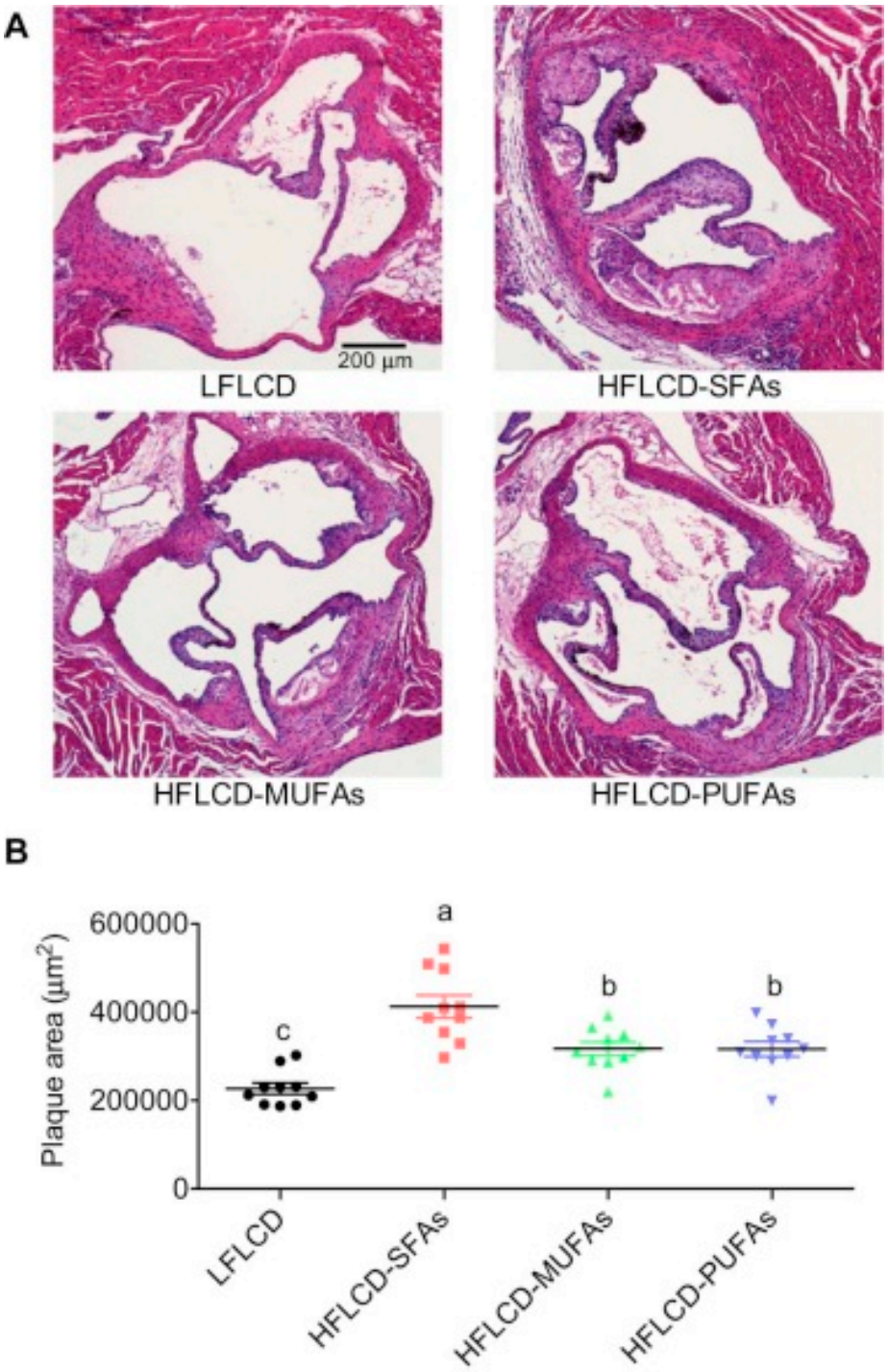
A
200 µm
LFLCD
HFLCD-SFAs
HFLCD-MUFAs
HFLCD-PUFAs
B
Plaque area (µm²)
600000
400000
200000
0
a
b
b
c
LFLCD
HFLCD-SFAs
HFLCD-MUFAs
HFLCD-PUFAs

Figure 3

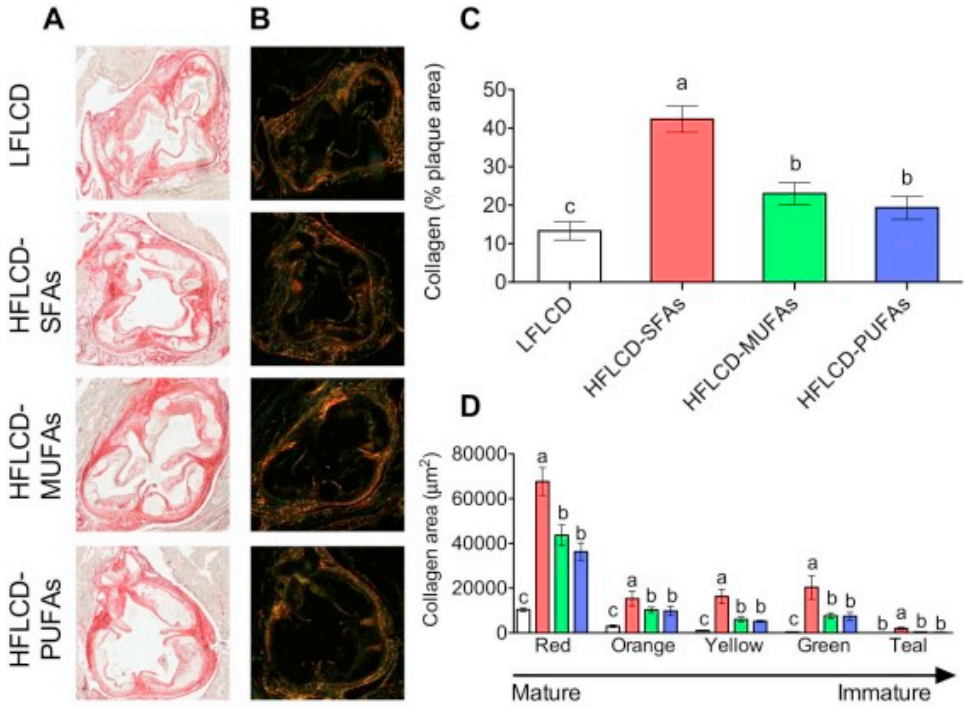
A
B
C
LFLCD
HFLCD-SFAs
HFLCD-MUFAs
HFLCD-PUFAs
Collagen (% plaque area)
50
40
30
20
10
0
a
b
b
c
LFLCD
HFLCD-SFAs
HFLCD-MUFAs
HFLCD-PUFAs
D
Collagen area (μm²)
80000
60000
40000
20000
0
Red
Orange
Yellow
Green
Teal
Mature
Immature

Figure 4

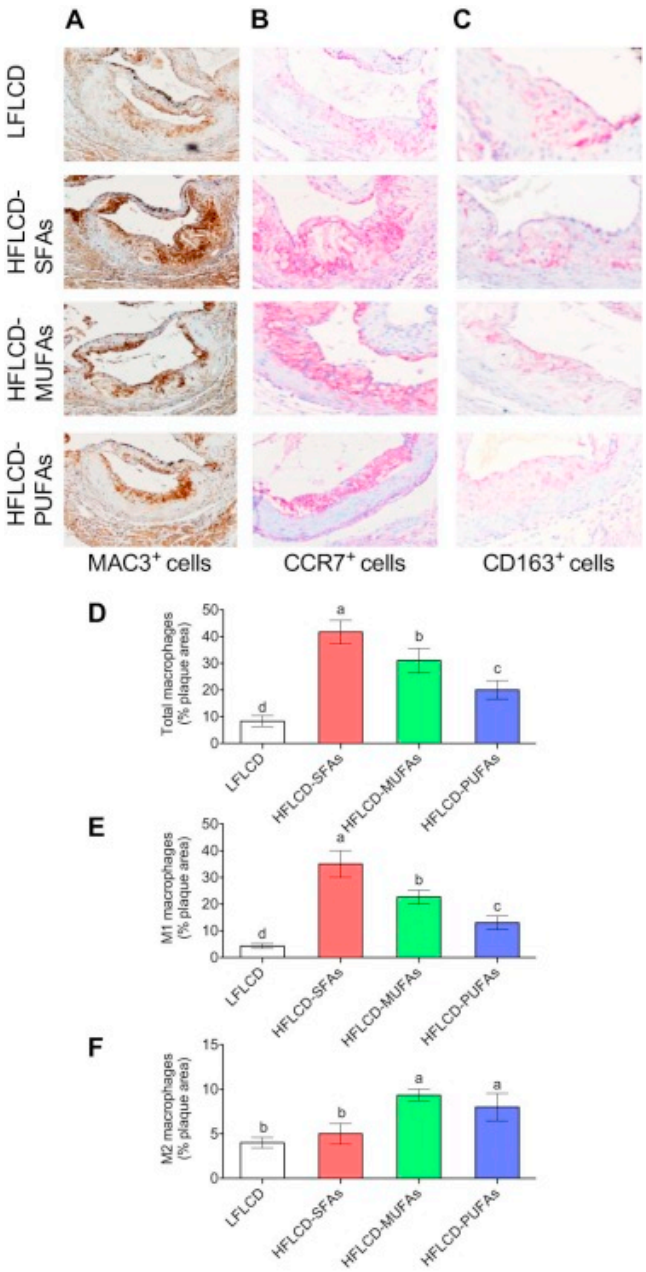
A
B
C
LFLCD
HFLCD-SFAs
HFLCD-MUFAs
HFLCD-PUFAs
MAC3+ cells
CCR7+ cells
CD163+ cells
D
Total macrophages (% plaque area)
E
M1 macrophages (% plaque area)
F
M2 macrophages (% plaque area)
LFLCD
HFLCD-SFAs
HFLCD-MUFAs
HFLCD-PUFAs